



# Extended Transfer Matrix Formalism Applied to Active Mach-Zehnder Interferometers with Built-in Semiconductor Optical Amplifiers

Yann G. Boucher<sup>(1)\*</sup> and Abdel-Fattah Fares<sup>(2)</sup>

<sup>(1)</sup> RESO Laboratory, ÉNIB, CS 73862, F-29238 Brest Cedex 3, France,

<sup>(2)</sup> Faculty of Electrical and Electronic Engineering, Aleppo University, Syria

\* Tel: 33 (0)298 05 66 66; Fax: 33 (0)298 05 66 89; E-mail: boucher@enib.fr

**Abstract-** We use an enlarged (5×5) Transfer Matrix Formalism to describe the linear and nonlinear properties of Mach-Zehnder Interferometers with built-in Semiconductor Optical Amplifiers. The active medium is subject to carrier saturation through both signal and Amplified Spontaneous Emission.

**Index Terms-** Amplified Spontaneous Emission (ASE), carrier saturation, Extended Transfer Matrix Formalism, Mach-Zehnder Interferometer (MZI), nonlinear optical function, Semi-conductor Optical Amplifier (SOA).

## I. INTRODUCTION

Active Mach-Zehnder Interferometers (MZI) with at least one Semiconductor Optical Amplifier (SOA) inserted in one of its arms have been largely proposed and investigated, notably in the context of the realization of all-optical functions. The insertion of active elements in such a device leads to several interesting consequences: in the linear regime, the signal can be simultaneously processed and amplified; besides, for a high enough level of input intensity, the carrier saturation inside the SOA can be taken advantage of, in order to realize nonlinear functions [1-5].

On the other hand, as soon as carriers are injected into the active region of the SOA (be it by electrical or optical pumping), Amplified Spontaneous Emission (ASE) is known to take place, leading to an additional noise which superposes itself to the input signal. Besides, ASE is also responsible for carrier saturation. Since the average car-

rier density  $N$  [m<sup>-3</sup>] inside the SOA determines not only the effective index (hence the phase) and the modal gain, but also the total rate of spontaneous emission, it is interesting to dispose of a unified description of all these effects at the scale of the whole MZI.

A few years ago, one of us has worked upon an extended Transfer Matrix Formalism (TMF) including sources (initially suggested by Weber & Wang for dealing with sources in periodic structures [6]), and applied it to the general study of spectral properties of ASE in SOA or in semiconductor lasers [7,8]. In what follows, we propose a simple and systematic description of a generalized active MZI with a SOA in each of its arms. Our enlarged (5×5) matrix formalism enables us to derive analytical expressions for the overall responses of such a device, with special emphasis on the properties of its own spontaneous emitted fields.

Our paper is organized as follows: in Section 2, we recall the main results relative to the extended (3×3) TMF as applied to an active SOA; Section 3 is devoted to the extended (5×5) transfer matrix of the MZI. Transfer functions are detailed in Section 4 on the specific example of a symmetrical MZI between two 50/50 couplers. The main trends and conclusions are summarized in Section 5.

## II. EXTENDED (3×3) TRANSFER MATRIX FORMALISM

The time dependence is taken as  $\exp(+i\omega t)$ . We limit ourselves to a scalar description of the electric field (for the sake of clarity, we neglect in this paper any polarization effects). The state of the field at any abscissa  $z$  along the propagation axis is completely determined by its propagative  $F^+$  and contra-propagative  $F^-$  parts [Fig. 1].



Fig. 1. Schematic representation of the relationship between input and output fields at both ends of an active structure.

The fields ( $F^+$ ,  $F^-$ ) at input abscissa  $z_0$  are related to the fields at output abscissa  $z_s$  by a (3×3) transfer matrix:

$$\begin{pmatrix} F_0^+ \\ F_0^- \\ 1 \end{pmatrix} = \begin{pmatrix} M_{11} & M_{12} & M_{13} \\ M_{21} & M_{22} & M_{23} \\ 0 & 0 & 1 \end{pmatrix} \begin{pmatrix} F_s^+ \\ F_s^- \\ 1 \end{pmatrix}, \quad (1a)$$

where the  $M_{ij}$  for  $(i, j) \in \{1, 2\}$  are that of the usual (2×2) TMF [9], whereas the  $M_{13}$  terms are related to the sources [6-8]. As a result, even when no input field is present ( $F_0^+ = F_0^- = 0$ ), background fields are nevertheless emitted:

$$B_s^+ \equiv F_s^+ = -(M_{13}/M_{11}), \quad (1b)$$

$$B_0^- \equiv F_0^- = (M_{23}M_{11} - M_{13}M_{21})/M_{11}. \quad (1c)$$

Let us consider a homogeneous single-pass SOA provided with ideal anti-reflection coating [Fig. 2]. The coefficients of its transfer matrix [A] between abscissas  $z_1$  and  $z_2$  are given by:

$$A_{11} = \exp(+i\beta_{\text{eff}}d) \exp(-g_{\text{mod}}d/2)/\eta^2, \quad (2a)$$

$$A_{12} = A_{21} = 0, \quad (2b)$$

$$A_{22} = 1/A_{11}, \quad (2c)$$

$$A_{13} = -\eta(u^+)A_{11}, \quad (2d)$$

$$A_{23} = -\eta[(u^+)A_{21} - (u^-)] = \eta(u^-), \quad (2e)$$

where  $\beta_{\text{eff}} = n_{\text{eff}}\omega/c$  denotes the real part of the wavevector,  $n_{\text{eff}}$  the effective index,  $g_{\text{mod}}$  the modal gain [ $\text{m}^{-1}$ ],  $d = z_2 - z_1$  the length of the active medium, and quality factor  $\eta$  accounts for possible insertion losses occurring from a modal mismatch between injected signal and SOA structure (for a typical 3 dB loss,  $\eta^2 = 0.5$ ).

Source terms ( $u^+$ ) and ( $u^-$ ) are the equivalent fields coupled to the optical mode at both ends [10]. They are defined through their average quadratic properties over the integration time of the detector, since their phase is a random value that cannot be determined experimentally.

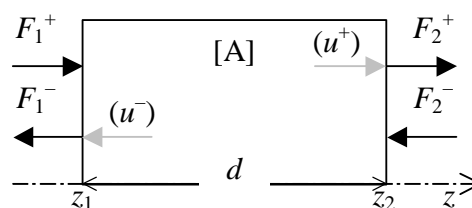


Fig. 2. ( $u^+$ ) and ( $u^-$ ) represent the equivalent fields of spontaneous emission coupled into the optical mode at both ends of the active section.

As soon as  $d$  is much greater than the wavelength, we get:

$$\langle |u^+|^2 \rangle = \langle |u^-|^2 \rangle, \quad (3a)$$

$$\langle u^+u^- \rangle \approx 0, \quad (3b)$$

where the brackets denotes the time average over the integration time of the detector under consideration. They can be related to the “intrinsic” spectral intensity  $I_U(\omega)$  generated in the active zone:

$$\begin{aligned} I_U(\omega) &= (\epsilon_0/2) c n_{\text{eff}} \langle |u^\pm|^2 \rangle \\ &= \beta_{\text{sp}} \hbar \omega r_{\text{sp}}(\omega) \frac{\exp(g_{\text{mod}}d) - 1}{g_{\text{mod}}}, \end{aligned} \quad (3c)$$

where  $r_{sp}(\omega)$  is the spectral rate of spontaneous emission and  $\beta_{sp}$  the fraction of spontaneous emission coupled into the optical mode [11].

All the optical properties of the active zone ( $n_{eff}$ ,  $g_{mod}$ ,  $r_{sp}$ ) are assumed to be completely determined by the mean carrier density  $N$  [ $m^{-3}$ ], which results from a balance between pumping and recombination processes, as expressed by the rate equation:

$$(dN/dt) = +\Lambda_p - R(N) - R_{SIG} - R_{ASE}, \quad (4a)$$

where  $\Lambda_p$  [ $m^{-3}\cdot s^{-1}$ ] denotes the pumping rate,  $R(N) = A N + B N^2 + C N^3$  the non-stimulated recombination,  $A$  [ $s^{-1}$ ] the non-radiative coefficient,  $B$  [ $m^3\cdot s^{-1}$ ] the spontaneous coefficient,  $C$  [ $m^6\cdot s^{-1}$ ] the Auger coefficient,  $R_{SIG}(N, P)$  the recombination stimulated by the signal, proportional to its photonic density  $P$ ,  $R_{ASE} (\propto N^2)$  the recombination stimulated by ASE. In steady-state regime, the equilibrium value of  $N$  is therefore completely fixed by two independent parameters:

$$N \equiv N(\Lambda_p, P). \quad (4b)$$

If we also assume that, in the range of interest at the signal wavelength,  $R_{SIG}$  can be written under the following linearized form:

$$R_{SIG} = B_{SIG} (N - N_0) P, \quad (4c)$$

then  $N$  is readily and explicitly obtained as the only physical solution of a mere polynomial equation of the third order.

### III. ACTIVE MACH-ZEHNDER INTERFEROMETER WITH SOA

The generic structure is depicted in Fig. 3. Without loss of generality, the input coupler is assimilated to a symmetrical directional linear coupler between two identical waveguides of wavevector  $\beta$ . It is completely determined by its dimensionless coupling constant  $\chi L$ . The input signal is

usually injected at port 1 from the left to the right, but the matrix relationship holds whatever the boundary conditions.

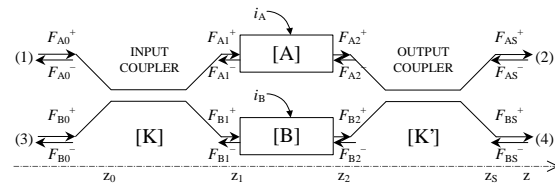


Fig. 3. Schematic depiction of the active MZI with built-in SOAs of transfer matrices [A] and [B], electrically pumped by current intensity  $i_A$  and  $i_B$ . Each passive coupler is represented by its transfer matrix [K] or [K'].

The output coupler is identical to the first except for its coupling constant  $\chi' L$ . Let us denote  $(F_A^+, F_A^-)$  the fields inside the upper waveguide, connecting ports 1 to 2, and  $(F_B^+, F_B^-)$  the fields inside the lower waveguide, connecting ports 3 to 4. The (5×5) transfer matrix [K] of an ideal passive linear coupler of coupling constant  $\chi L$  is such as:

$$\begin{pmatrix} F_{A0}^+ \\ F_{A0}^- \\ F_{B0}^+ \\ F_{B0}^- \\ 1 \end{pmatrix} = \begin{bmatrix} \tau & 0 & \kappa & 0 & 0 \\ 0 & \tau^* & 0 & \kappa^* & 0 \\ \kappa & 0 & \tau & 0 & 0 \\ 0 & \kappa^* & 0 & \tau^* & 0 \\ 0 & 0 & 0 & 0 & 1 \end{bmatrix} \begin{pmatrix} F_{A1}^+ \\ F_{A1}^- \\ F_{B1}^+ \\ F_{B1}^- \\ 1 \end{pmatrix}, \quad (5a)$$

with  $\tau = e^{i\beta L} \cos(\chi L)$  and  $\kappa = e^{i\beta L} i \sin(\chi L)$ .

The (5×5) transfer matrix [K'] of the output coupler is obtained in a similar fashion. The (5×5) transfer matrix [G] of the central gain zone reads:

$$[G] = \begin{bmatrix} A_{11} & A_{12} & 0 & 0 & A_{13} \\ A_{21} & A_{22} & 0 & 0 & A_{23} \\ 0 & 0 & B_{11} & B_{12} & B_{13} \\ 0 & 0 & B_{21} & B_{22} & B_{23} \\ 0 & 0 & 0 & 0 & 1 \end{bmatrix}. \quad (5b)$$

Now the total (5×5) matrix [M] of the active

MZI, with [A] in the upper arm and [B] in the lower arm between couplers [K] and [K'], is:

$$[M] = [K] [G] [K']. \quad (5c)$$

Without loss of generality, for the ideal single-pass SOAs, we can write:

$$A_{11} = 1/A_{22} = \exp(+i \Phi_A) \exp(-\Gamma_A), \quad (6a)$$

$$A_{12} = A_{21} = 0, \quad (6b)$$

$$A_{13} = -\eta(u_A^+) A_{11}, \quad (6c)$$

$$A_{23} = +\eta(u_A^-), \quad (6d)$$

$$B_{11} = 1/B_{22} = \exp(+i \Phi_B) \exp(-\Gamma_B), \quad (6e)$$

$$B_{12} = B_{21} = 0, \quad (6f)$$

$$B_{13} = -\eta(u_B^+) B_{11}, \quad (6g)$$

$$B_{23} = +\eta(u_B^-), \quad (6h)$$

where  $\Phi_A$  (resp.  $\Phi_B$ ) represents the overall phase on the upper (resp. lower) arm,  $\Gamma_A$  (resp.  $\Gamma_B$ ) the overall dimensionless amplification coefficient.

Note that we are interested mostly in fields  $F^+$  propagating from the left to the right. If  $F_{B0}^+ = 0$ , the input fields in both SOAs at abscissa  $z_1$  are given as a function of  $F_{A0}^+$  by:

$$F_{A1}^+ = F_{A0}^+ \cos(\chi L) \exp(-i \beta L), \quad (7a)$$

$$F_{B1}^+ = -i F_{A0}^+ \sin(\chi L) \exp(-i \beta L). \quad (7b)$$

The fraction of power coupled across the coupler is  $\cos^2(\chi L)$  on one path,  $\sin^2(\chi L)$  on the other. The input signal in each SOA being known, it becomes possible to determine the (average) photonic densities ( $P_A$ ,  $P_B$ ) that, along with ASE, contribute to carrier saturation. Once the carrier densities ( $N_A$ ,  $N_B$ ) are determined according to eqn.(4b), a straightforward calculation leads to:

$$F_{A2}^+ = F_{A1}^+ \exp(-i \Phi_A + \Gamma_A) + \eta(u_A^+), \quad (7c)$$

$$F_{B2}^+ = F_{B1}^+ \exp(-i \Phi_B + \Gamma_B) + \eta(u_B^+), \quad (7d)$$

These two fields represent the input fields at abscissa  $z_2$  on the second (output) coupler [K']. The index (A or B) obviously relates to one or the other SOA. As a result, fields emitted at both ports (2) and (4) at abscissa  $z_S$  are expressed as linear combinations of  $F_{A2}^+$  and  $F_{B2}^+$ :

$$\begin{aligned} F_{AS}^+ &= [\cos(\chi L) F_{A2}^+ - i \sin(\chi L) F_{B2}^+] e^{-i \beta L}, \\ F_{BS}^+ &= [-i \sin(\chi L) F_{A2}^+ + \cos(\chi L) F_{B2}^+] e^{-i \beta L}. \end{aligned} \quad (7e,f)$$

We would like to emphasize that spontaneous emission terms ( $u_A^+$ ) and ( $u_B^+$ ) that appear in the developed expression of both output fields ( $F_{AS}^+$ ,  $F_{BS}^+$ ) are non coherent with the signal, and non coherent mutually. They add in intensity.

#### IV. EXAMPLE OF A SYMMETRICAL ACTIVE MZI WITH SOA

For the sake of clarity, let us consider a system with two identical 50/50 couplers:  $[K] = [K']$ ,  $\chi L = \pi/4$ ,  $\cos^2(\chi L) = \sin^2(\chi L) = 1/2$ . A straightforward calculation leads to the following expression for the overall (5×5) transfer matrix:

$$[M] = \begin{bmatrix} M_{11} & 0 & M_{13} & 0 & M_{15} \\ 0 & M_{22} & 0 & M_{24} & M_{25} \\ M_{31} & 0 & M_{33} & 0 & M_{35} \\ 0 & M_{42} & 0 & M_{44} & M_{45} \\ 0 & 0 & 0 & 0 & 1 \end{bmatrix}, \quad (8a)$$

$$M_{11} = -M_{33} = i \exp(i \Psi_0) \sin(\Delta \Psi), \quad (8b)$$

$$M_{13} = M_{31} = i \exp(i \Psi_0) \cos(\Delta \Psi), \quad (8c)$$

$$M_{22} = -M_{44} = -i \exp(-i \Psi_0) \sin(\Delta \Psi), \quad (8d)$$

$$M_{24} = M_{42} = -i \exp(-i \Psi_0) \cos(\Delta \Psi), \quad (8e)$$

where "phases" are complex numbers:

$$\Psi_0 = \Psi_m + 2 \beta L, \quad (9a)$$

$$\Psi_m = (\Psi_A + \Psi_B)/2, \quad (9b)$$

$$\Psi_A = \Phi_A + i \Gamma_A, \quad (9c)$$

$$\Psi_B = \Phi_B + i \Gamma_B, \quad (9d)$$

$$\Phi = (\Phi_A + \Phi_B)/2, \quad (9e)$$

$$\Gamma = (\Gamma_A + \Gamma_B)/2, \quad (9f)$$

$$\Delta \Psi = (\Psi_A - \Psi_B)/2, \quad (9g)$$

$$\Delta \Phi = (\Phi_A - \Phi_B)/2, \quad (9h)$$

$$\Delta \Gamma = (\Gamma_A - \Gamma_B)/2, \quad (9i)$$

and the source terms read:

$$M_{15} = (\sqrt{2}/2) e^{+i \beta L} [A_{13} + i B_{13}], \quad (10a)$$

$$M_{25} = (\sqrt{2}/2) e^{-i\beta L} [A_{23} - i B_{23}], \quad (10b)$$

$$M_{35} = (\sqrt{2}/2) e^{+i\beta L} [+i A_{13} + B_{13}], \quad (10c)$$

$$M_{45} = (\sqrt{2}/2) e^{-i\beta L} [-i A_{23} + B_{23}]. \quad (10d)$$

Under a more explicit form:

$$M_{15} = -(\eta / \sqrt{2}) e^{i\beta L} [(u_A^+) e^{i\Psi_A} + i(u_B^+) e^{i\Psi_B}],$$

$$M_{25} = -(\eta / \sqrt{2}) e^{-i\beta L} [-(u_A^-) + i(u_B^-)],$$

$$M_{35} = -(\eta / \sqrt{2}) e^{i\beta L} [i(u_A^+) e^{i\Psi_A} + (u_B^+) e^{i\Psi_B}],$$

$$M_{45} = -(\eta / \sqrt{2}) e^{-i\beta L} [i(u_A^-) - (u_B^-)].$$

If  $F_{B0}^+ = 0$ , the emitted spectral intensity on ports (2) and (4) [ $\text{W}\cdot\text{m}^{-2}\cdot\text{Hz}^{-1}$ ], respectively proportional to  $\langle |F_{AS}^+|^2 \rangle$  and  $\langle |F_{BS}^+|^2 \rangle$ , are:

$$I_{AS}^+ = T_{AA} I_{A0}^+ + \eta^2 I_U, \quad (11a)$$

$$I_{BS}^+ = T_{BA} I_{A0}^+ + \eta^2 I_U, \quad (11b)$$

$$T_{AA} = e^{2\Gamma} [\cosh(2\Delta\Gamma) - \cos(2\Delta\Phi)]/2, \quad (11c)$$

$$T_{BA} = e^{2\Gamma} [\cosh(2\Delta\Gamma) + \cos(2\Delta\Phi)]/2. \quad (11d)$$

If ideal phase sections (devoid of gain and sources) replace active SOAs, we recover on both paths the complementary responses of an ideal MZI ( $T_{AA} + T_{BB} = 1$ ) [Fig. 4].

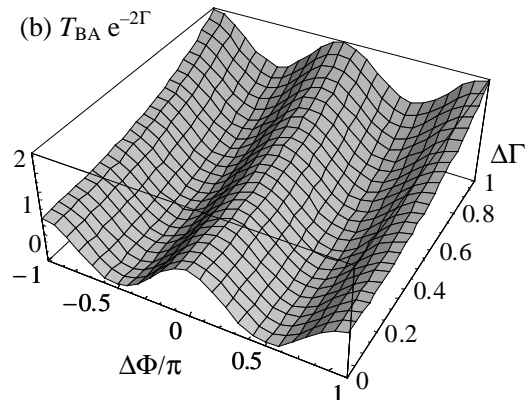
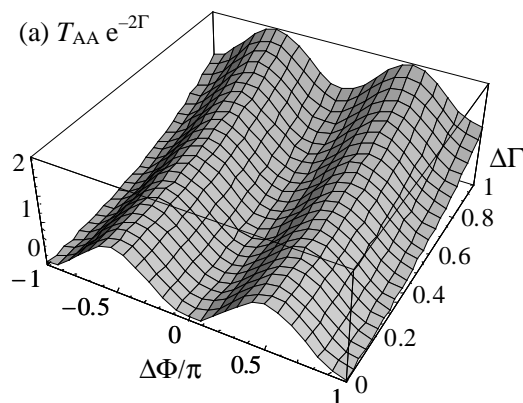


Fig. 4. Direct and cross transfer functions:

$$(a) T_{AA} \exp(-2\Gamma) = [\cosh(2\Delta\Gamma) - \cos(2\Delta\Phi)]/2,$$

$$(b) T_{BA} \exp(-2\Gamma) = [\cosh(2\Delta\Gamma) + \cos(2\Delta\Phi)]/2.$$

With built-in SOAs, signal is not only transmitted and amplified with transfer functions  $T_{AA}$  or  $T_{BA}$ : output intensity also carries an extra contribution ( $\eta^2 I_U$ ) coming from ASE. We would like to emphasize that the amount of spontaneous “offset” strongly depends on the spectral characteristics of the following detector: with a narrow filter suitably centered on the signal wavelength, the background noise can be made negligible.

Between two identical (50/50) couplers, if the two arms are perfectly balanced ( $\Delta\Phi = \Delta\Gamma = 0$ ), then  $T_{AA} = 0$  and  $T_{BA} = \exp(2\Gamma)$ . For the sake of illustration, let us consider an asymmetrical carrier density around an average value  $N_m$ :  $N_A = N_m + \Delta N$ ,  $N_B = N_m - \Delta N$ . For a 500  $\mu\text{m}$  long SOA at 1.5  $\mu\text{m}$ , typical variations are  $(\partial\Phi/\partial N) \equiv -10^{-23} \pi \text{ m}^3$ ,  $(\partial\Gamma/\partial N) \equiv +10^{-24} \text{ m}^3$ . Simulations drawn on Fig. 5 show the effect, on both transfer functions, of the differential carrier density.

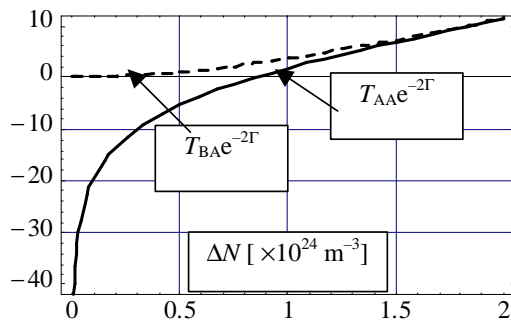


Fig. 5.  $T_{AA} \exp(-2\Gamma)$  and  $T_{BA} \exp(-2\Gamma)$  [dB], with  $(\partial\Gamma/\partial N) \equiv +10^{-24} \text{ m}^3$ ,  $(\partial\Phi/\partial N) \equiv -10^{-23} \pi \text{ m}^3$ .

In this particular example, the system is almost insensitive to nonlinear effects, since the optically induced variations of carrier density in both SOAs (submitted to the same optical power) compensate each other. With such a choice of material parameters, the state of interference would be hardly affected. Note that a phase shift section (driven by an independent control current) can be added on one path outside the SOA [12]: our formalism remains perfectly suited.

Besides, if we were to realize all-optical nonlinear functions, it would be enough to choose an unbalanced input coupler, since an unequal repartition of power would be required. Our formalism would remain exactly the same, except for  $\chi L \neq (\pi/4)$ .

## V. CONCLUSION

Extended (5×5) Transfer Matrix Formalism appears well adapted to the description of active MZI with built-in SOAs. We obtain easily the nonlinear responses of the system in a self-consistent way, taking into account the carrier saturation (in the active medium) by both signal and ASE. Direct and cross transfer functions are expressed in the spectral domain, spontaneous emission included. The time response is essentially limited by carrier dynamics.

In short, extended TMF provides exactly the same kind of information as usual TMF without

sources, with the added advantages that it enables one to:

*i* / describe the background output field even when no input field is injected;

*ii* / evaluate the spectral density of ASE in each active zone;

*iii* / calculate the total amount of carrier recombination stimulated by ASE;

*iv* / determine the precise steady-state value of carrier density in each SOA.

It should be noted that a mere (4×4) TMF would systematically underestimate the total recombination rate, thus overestimating the equilibrium value of carrier density.

It should also be noted that, as an alternative, the active properties of the system seen as a 4-port network can also be expressed through an extended (5×5) scattering matrix, provided with an added fifth column that contains the “background” source terms:  $S_{15} = B_{A0}^-$ ,  $S_{25} = B_{AS}^+$ ,  $S_{35} = B_{B0}^-$ ,  $S_{45} = B_{BS}^+$ . As a matter of fact, although we have limited ourselves to an ideal unidirectional configuration, ASE is actually emitted both ways: we would like to emphasize that our extended TMF would naturally take into account bidirectional transmission schemes with various boundary conditions, such as pump-probe configurations. Besides, it remains general enough to include non-ideal SOA with poor anti-reflection coating: the transfer matrices [A] and [B] would simply exhibit non-diagonal elements. It can also be applied to other kinds of generalized MZI configurations, including built-in active or passive resonators, nonlinear Fabry-Perot cavities, periodic structures and so on.

## ACKNOWLEDGMENT

This work was supported in part by the Syria Ministry of Higher Education. The authors would

also like to express their gratitude to Pr. Le Bihan, Head of RESO Laboratory at École Nationale d'Ingénieurs de Brest, France, for his support and encouragement, as well as Pr. Sharaiha and Dr. Guégan for helpful discussions

## REFERENCES

- [1] T. Durhuus, C. Joergensen, B. Mikkelsen, R.J.S. Pedersen, K.E. Stubkjaer, "All Optical Wavelength Conversion by SOA's in a Mach-Zehnder Configuration", *IEEE Photon. Technol. Lett.*, Vol. 6 (1), pp. 53–55, 1994.
- [2] L.H. Spiekman, J.M. Wiesenfeld, U. Koren, B.I. Miller, M.D. Chien, "All-Optical Mach-Zehnder Wavelength Converter with Monolithically Integrated Preamplifiers", *IEEE Photon. Technol. Lett.*, Vol. 10 (8), pp. 1115–1117, 1998.
- [3] E.A. Patent, J.J.G.M. van der Tol, R.G. Broeke, J.J.M. Binsma, "Semiconductor Optical Amplifiers in a non-linear Mach-Zehnder Interferometer", in *Proc. Symposium IEEE/LEOS Benelux Chapter*, Amsterdam, 2002, s02p58.
- [4] R. Ngah, Z. Ghassemlooy and G. Swift, "Comparison Of Interferometric All-Optical Switches For Router Applications In OTDM Systems", in *Fourth Annual Postgraduate Symposium on Convergence of Telecommunications, Networking and Broadcasting*, Liverpool (UK), June 2003, pp. 81–85 [ISBN: 1-9025-6009-4 © 2003 PGNet].
- [5] M.J. Connelly, "Semiconductor Optical Amplifiers and their Applications", presented at *IASTED International Conference on Optical Communications Systems and Networks (OCSN 2005)*, Banff, Canada – tutorial, July 2005.
- [6] J.-P. Weber, S. Wang, "A New Method for the Calculation of the Emission Spectrum of DFB and DBR Lasers", *IEEE J. Quantum Electron.*, Vol. 27 (10), pp. 2256–2266, 1991; J.-P. Weber, "Correction to "A New Method for the Calculation of the Emission Spectrum of DFB and DBR Lasers"", *IEEE J. Quantum Electron.*, Vol. 29 (1), p. 296, 1993.
- [7] Y. Boucher, A. Sharaiha, "Spectral Properties of Amplified Spontaneous Emission in Semiconductor Optical Amplifiers", *IEEE J. Quantum Electron.*, Vol. 36 (6), pp.708–720, 2000.
- [8] Y. Boucher, "Extended (3×3) Transfer Matrix Formalism: From Amplified Spontaneous Emission to Threshold-Crossing", *Research Signpost: Recent Res. Devel. in Optics* (3), pp.177–204, 2003.
- [9] A. Yariv & P. Yeh, *Optical Waves in Crystals*, Wiley, New York, 1984.
- [10] H.K. Choi, K.L. Chen, S. Wang, "Analysis of Two-Section Coupled-Cavity Semiconductor Lasers", *IEEE J. Quantum Electron.*, Vol. QE-20 (4), pp. 385–393, 1984.
- [11] G.P. Agrawal, N.K. Dutta, *Long Wavelength Semiconductor Lasers*, Van Nostrand Rheinhold, New York, 1986.
- [12] G. Morthier, J. Sun, T. Gyselings and R. Baets, "A Novel Optical Decision Circuit Based on a Mach-Zehnder or Michelson Interferometer and Gain-Clamped Semiconductor Optical Amplifiers", *IEEE Photon. Technol. Lett.*, Vol. 10 (8), pp. 1162–1164, 1998.